An adaptive gaze stabilisation controller inspired by the vestibulo-ocular reflex

A. Lenz, T. Balakrishnan, A. G. Pipe and C. Melhuish

Bristol Robotics Laboratories, University of Bristol & University of the West of England, Bristol Business Park, Coldharbour Lane, Bristol, BS16 1QY, GB

E-mail: alex.lenz@brl.ac.uk

Abstract.

The vestibulo-ocular reflex stabilises vision in many vertebrates. It integrates inertial and visual information to drive the eyes in the opposite direction to head movement and therefore stabilises the image on the retina. Its adaptive nature guarantees stable vision even when the biological system undergoes dynamic changes (due to disease, growth or fatigue etc.), a characteristic especially desirable in autonomous robotic systems. Based on novel, biological plausible neurological models, we have developed a robotic testbed to qualitatively evaluate the performance of these algorithms. We show how the adaptive controller can adapt to a time varying plant and elaborate how this biologically inspired control architecture can be employed in general engineering applications where sensory feedback is very noisy and/or delayed.

1. Introduction

Mobile agents, whether natural or artificial, are all faced with the problem of disturbances with respect to their vision system while moving. This phenomenon is easily observed when looking at, typically shaky, video footage shot with a hand-held camera whilst walking. By decoupling the vision system, the eye, from the main body or head, nature has come up with an efficient way of tackling the crucial task of gaze stabilisation.

Insects, featuring fixed compound eyes, move their head relative to their body when encountering disturbances during flight. Many vertebrates (from goldfish to humans) are, on the other hand, able to rotate their eyes relative to their head via extraocular muscles.

The mechanism that stabilises vision in these animals with respect to rotations and translations of their head is referred to as the vestibulo-ocular reflex (VOR). This reflex drives the eyes in the opposite direction to the head movement and consequently preserves the image in the centre of the retina [1], [2].

The VOR does not use the very slow visual feedback to drive the eyes, in fact it works well in complete darkness. As its name implies, it uses the vestibular system of the inner ear to sense head rotations and transversal movements to generate a motor signal to counter-rotate the eyes. However, in the context of this paper only the rotational VOR is addressed and transversal head movements are not considered.

1.1. Biological Inspiration

Very early in the history of neuroscience the VOR was identified as a three neuron arc (e.g. R. Magnus, 1924 Körperstellung). The head rotation is sensed by the vestibular system and this information is passed on to interneurons in vestibular nuclei in the brainstem. From here the signal, after some integration, is further relayed on to the motor neurons which induce muscle contraction.

From an engineering perspective it is clear that such a feed-forward system requires calibration. The sensitivity of the sensory system does not necessarily produce signal magnitudes to supply the muscles with the necessary inputs. Furthermore, stable gaze can only be achieved if the dynamic components of the sensory and motor system are compensated for by the brainstem feed-forward filter.

Considering that biological systems are often time varying due to injury, disease, or aging, a need for constant calibration/adaptation becomes apparent. The visual slip, i.e. the degree of movement of the eye's lens projection on the retina, not only gives a good measure of how well the system has adapted but also provides an appropriate teaching signal for the adaptive structures. However, since the visual slip signal arrives at the relevant neural structures with a delay of approximately 100ms, it can not be used as a direct feedback signal to generate eye movements.
A range of animal experiments with magnifying lenses and vision distorting prisms has been performed. It has been shown that artificially induced visual slip is compensated

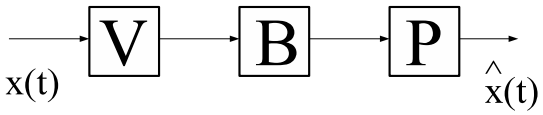

Figure 1. The 3-Neuron-Arc (one-dimensional example); in a perfectly tuned system the magnitude of the transfer function ($\frac{\widehat{x(t)}}{x(t)} = V \cdot B \cdot P$), which describes the eye velocity in relation to the head velocity, equals 1; (V denotes the vestibular system, B the brainstem and P the oculo-motor plant.)

for by the neural system and that the adaptation takes place over several hours and is reversible when the distorting devices are removed. For a review of the experimental data see Broussard [3].

The neural structure responsible for this adaptation is the cerebellum. In terms of evolutionary development, this older part of the brain is widely understood [4] to act as an adaptive filter which can be used to fine-tune motor commands based on inadequacies of current performance. This is not only true for the VOR but all other aspects of joint motor control. Early models by Marr [5] and Albus [6] already describe the cerebellum from such a perspective. Ito [7] identified the cerebellar microcircuit and showed that it has a very regular structure, which is evident throughout the cerebellar cortex.

Despite the fact that there is some disagreement over the details of this plasticity in the case of the VOR, a few facts are generally agreed on: (i) an intact cerebellar cortex is required; (ii) vision, in combination with another signal, is necessary; (iii) the second signal can be vestibular or oculomotor and (iv) lability and reversibility depend on exact conditions and temporal order of both.

1.2. Recurrent Decorellation Control

Dean [8] introduced the concept of decorrelation control as a plausible model for plasticity of the VOR in April 2002. In a paper following up this initial work, Porrill and Dean [9] argue that the application of decorrelation control in a recurrent architecture is an appropriate learning paradigm in a multi-degree of freedom system and differs significantly from Kawato's ([10]; [11]) well known model of feedback-error-learning. Figure 2 outlines Dean's and Porrill's ideas. The VOR neural circuit differs from classical adaptive control architecture by having the information flow through the adaptive element (the cerebellum) reversed, i.e., a copy of the motor command is fed back through the cerebellum and the cerebellar output is added to the sensory input. In other words, the cerebellum, in conjunction with the brainstem, forms a recurrent system. This is in line with anatomical and electrophysiological evidence. To be more precise, in the biological system the cerebellar output is an inhibitory signal which could have been reflected in subtracting the cerebellar contribution from the sensory input. However, for mathematical convenience we choose this additive structure which has no consequences for the generality of our solution from a signal processing point of view.

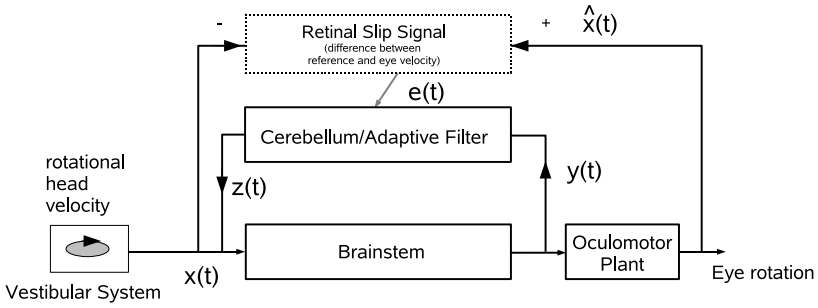

Figure 2. Recurrent architecture of a biologically plausible adaptive VOR controller: the head velocity is sensed by the vestibular system and added to the cerebellar output. The signal is then passed on to the brainstem and acts as a motor command for the oculomotor system. A copy of this motor command is sent back to the cerebellum. The difference between head and eye rotation is perceived as visual slip, which is another input signal into the cerebellum.

In a sufficiently tuned system the brainstem, in conjunction with the cerebellar microcircuit, act as an inverted oculomotor plant and consequently the retinal slip signal is reduced to a minimum. In other words, the gaze is stable while the head experiences rotational perturbations.

1.3. Cerebellar Control Structure

A small part of the cerebellar cortex performing this partial plant inversion is schematically shown in figure 3. Its functionality, for our proposed model of VOR motor learning, can be understood as follows: The motor command arrives at the cortex via the mossy fibres which synapse on the granule cells whose axons form parallel fibres (PF). The parallel fibres synapse on the huge dendritic tree of the Purkinje cells (PC). The (inhibitory) output of the Purkinje cell projects back to the brainstem. Each Purkinje cell is innervated by a climbing fibre which carries the error signal (i.e. visual slip) from the inferior olive. Correlated firing of parallel fibres and climbing fibres alters the synaptic efficacy of the PF-PC synapses and therefore alters the transfer function of the signal flow from the mossy fibre input to the Purkinje cell output.

Clearly, the cerebellar microzone is a complex biological system which could be modelled at different levels of abstraction. Similarly, the brainstem, the extraocular muscles and the semicircular canals could be replicated to arbitrary levels of biological plausibility. However, in order to test the functionality of the recurrent control structure in principle, a linear system approach is not only sufficient but also provides us with the ability to analyse the performance with ease.

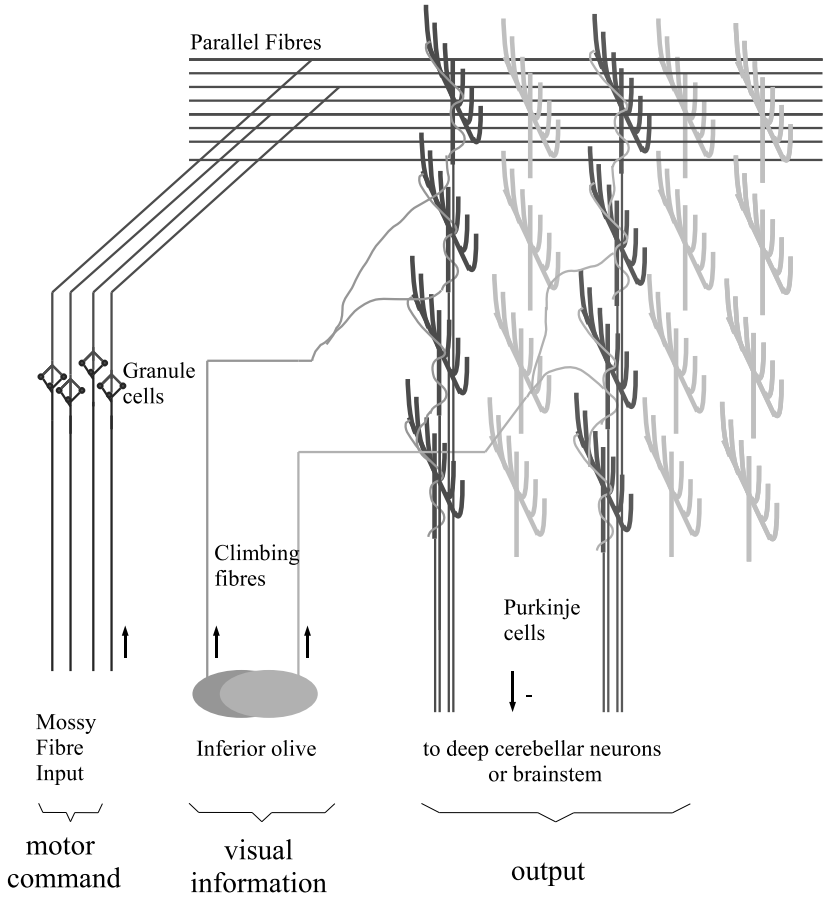

Figure 3. Geometry of mossy and parallel fibre system and the connectivity of Purkinje cells and climbing fibres

2. System Modelling and Design

Under real-life conditions, the VOR comprises the concerted operation of numerous parallel pathways. The three semicircular canals and two otolith organs in each labyrinth, associated with the left and right inner ear, form ten separate input signals. Each eye is rotated about three axis of freedom (yaw, pitch and roll) by three pairs of antagonistic muscles.Considering both eyes, this results in twelve individual muscles driven with precise and well timed motor commands.

For our robotic implementation we focus on the yaw (rotation in the horizontal plane) movements of a single eye for the initial test of the algorithmic structure. However, the equipment we have designed is laid out for extension to 3-dimensional rotations. The time constants and gains of the following models are adapted from Porrill [9].

2.1. Linear System models

The vestibular system is assumed to provide the brainstem with an accurate representation of the rotational velocity.

The brainstem is modelled as a first order leaky integrator plus a pure DC gain. It's transfer function models the production of a motor command from the sensory input of the vestibular system. The Laplace transform of the brainstem model is shown in equation 1.

$$B(s) = G_d + \frac{G_I}{s + \frac{1}{T_I}}, \tag{1}$$

with $G_d = 1.05$, $G_I = 2.5$ and $T_I = 1s$.

The first order dynamic model of the oculomotor plant transforms the intensity of the muscle innervation into a rotational velocity. Again, the model is presented here as a Laplace transform in equation 2.

$$P(s) = \frac{s}{s + \frac{1}{T_P}}, \tag{2}$$

with a time constant T_P of 0.1s.

As an illustration, the response of both the brainstem model and the oculomotor plant to a sudden step change to their inputs is shown below.

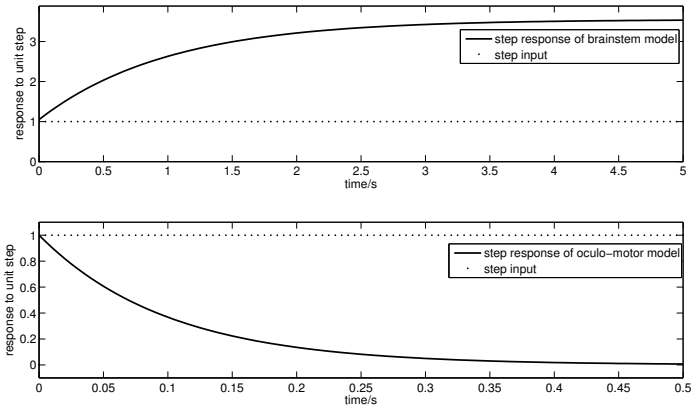

Figure 4. The plot on the top shows the step response of the brainstem model (see also equation 1). The step response of the oculomotor plant model is presented in the bottom plot (see also equation 2)

The cerebellum is implemented as an adaptive FIR (finite impulse response) filter comprising a delay line with 200 taps.

$$z(t) = \sum_{i=0}^{199} w_i y(t - i \cdot \Delta T), \tag{3}$$

where $\Delta T = 0.01s$ is the time delay between the filter taps, w_i are the filter weights and $y(\cdot)$ is the filter input history. See also figure 13 for an illustration of this filter structure.

2.2. Robotic Components

2.2.1. Artificial Vestibular System To measure angular velocities in three axes we employ three MEMS gyroscopes from Analog Devices^{TM}, the ADXRS300 (see figure 5). The output of this device is a voltage proportional to the angular velocity about the axis normal to the top surface of the device (yaw rate sensor). The chip employs the displacement of a resonating mass orthogonally to its direction of motion due to coriolis acceleration experienced when rotating.‡ The advantage of such a design in comparison to linear accelerometers is that the output is independent of the position of the device on the rotating object as long as the axis of sensing is parallel to the axis of rotation.

The chosen device features a full scale range of $\pm 300°/s$ and a sensitivity of $5mV/(°/s)$. The bandwith is 40Hz.

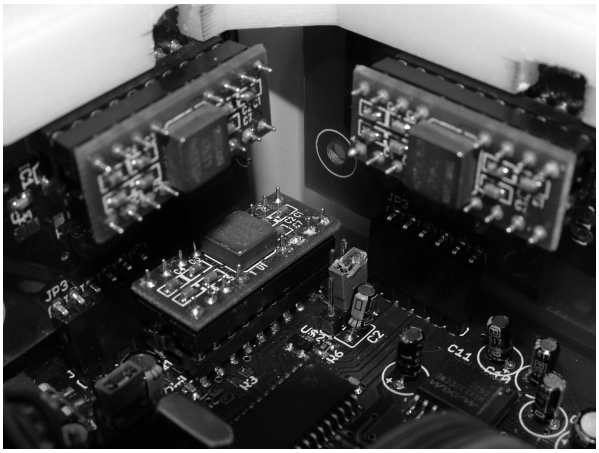

Figure 5. The three MEMS gyroscopes mounted in a mutually orthogonal setup.

We employ a dsPIC30F3013 microcontroller from Microchip^{TM}to sample the three rotational velocities, perform a 12-bit analog to digital conversion and provide SPI and RS232 interfaces for accessing the rotational velocities. This approach not only provides us with a clean modular design with defined interfaces, but also ensures local computational power which could be used in future to transform the sensed rotational velocities of the engineered vestibular system into more biologically plausible signals.

2.2.2. Artificial Oculomotor System We constructed an artificial eye system which allows a gimbal mounted camera to be moved with three degrees of freedom (see figure 6).

‡ $a_{coriolis} = 2\omega \times v$; with ω being the angular velocity of the system and v the current velocity of the resonating mass.

Each axis of rotation is driven by a brushless DC motor with a custom designed gearbox (gear ratio 1:36; timing belt mechanism in order to avoid backlash problems).

When using an electrical motor to substitute muscles in an artificial system, an immediate problem arises due to their different dynamic characteristics. When employing a simple first order dynamic model and looking at the step response of the (rotational) velocity of both systems, the difference becomes apparent (see figure 7). Whereas an electrical motor accelerates and reaches a constant velocity for $t \longrightarrow \infty$, our simple oculomotor model, proposed in equation 2, reaches its maximum velocity immediately after innervation and slows down over time, reaching a rotational velocity of zero for $t \longrightarrow \infty$.

To overcome this problem and to enable us to employ different plant dynamics when testing our algorithms, we adopt the following scheme for each axis:

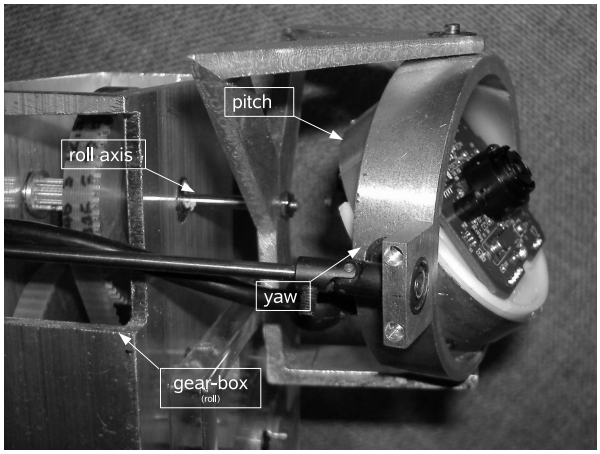

Figure 6. Photograph of the gimbal mounted camera system. The inner ring rotates around the pitch axis, the next ring around yaw and the outer ring generates the roll movements. The pushrod for yaw is visible in the foreground. The pushrod for pitch is removed on this photograph.

The brushless DC motor is driven by a microcontroller. We opted for the dsPIC30F4012, a 16 bit microcontroller from Microchip ™, which is ideally suited for motor control applications, providing interfaces for incremental encoders, and multiple PWM output units. The current angular position is constantly sensed using an incremental encoder. A closed-loop PID controller is implemented to control the velocity of the motor. A well tuned and fast controller enables us to assume an almost perfect ($v(t) = v_0 \cdot \epsilon(t)$) velocity step response of our brushless DC motor system. Consequently, we are able to emulate muscle-like dynamics by employing a digital filter describing these dynamics in series with the closed-loop controller (see figure 8). All this is implemented locally and can be done independently for each axis.

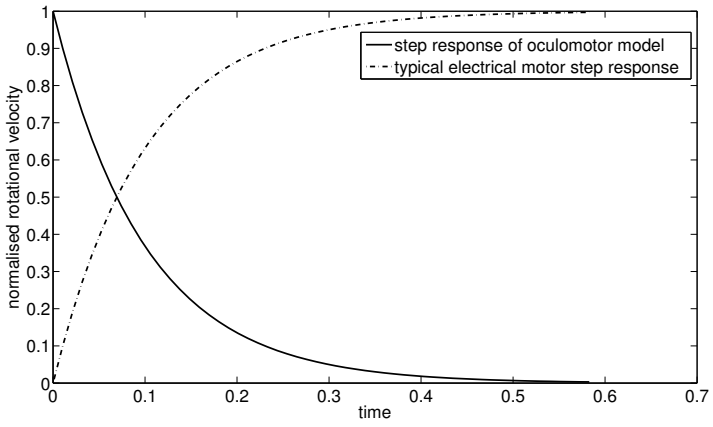

Figure 7. Normalised velocity step response of a first order muscle and electrical motor model with equal time constants.

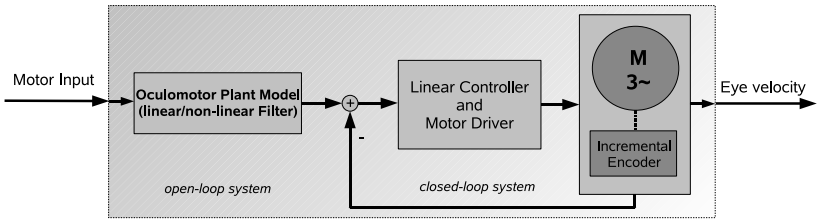

Figure 8. Motor controller with filter enables us to emulate 'arbitrary' plant dynamics

2.2.3. Vision System The vision system is greatly simplified in comparison to a more biologically plausible one. We chose a simple webcam§ embedded in the centre of the eye mechanism as can be seen in figure 6. The camera monitors a laser projection on a monochrome background. A simple frame comparison algorithm finds the position (in frame coordinates) of the projection (simply the area of the highest light intensity) for each frame and derives the magnitude of the image flow for the x and y coordinates.

Our C++ vision software runs on standard Windows^{TM}PC and the camera is connected via USB2.0‖. The software interface to the camera settings and the access to the data of each frame is achieved by employing the *Intel Open Source Computer Vision Library* (openCV).

2.2.4. Systems Integration In a final step to connect the developed components, we created an embedded computing platform based around the dsPIC30F6012^{TM}microcontroller. This board provides several interfaces (RS232, CAN, SPI and general purpose digital I/O) which enable our modular design to be integrated and tested. Furthermore, the microcontroller's fixed-point RISC kernel provides suffi-

§ Logitech^{TM}QuickCAM Pro 5000, 640 × 480 pixel, at 30 frames per second

‖ The Universal Serial Bus (USB) is a 4 wire (power, ground, 2x data) serial bus standard to interface external devices to personal computers. In its high-speed variety it provides data rates up to 480 Mbit/s

cient computational throughput to run the cerebellar inspired learning algorithm.

Figure 9 shows the interfacing of the motor-system via a Controller Area Network (CAN)¶. All dynamic states of the system are broadcast on the CAN and we are able to observe those via a custom designed PC software interface.

The gyroscope is integrated via SPI, its sensory information being polled on a regular basis. The vision processing is performed on a PC and only the visual motion along the x and y axis is conveyed via a low-bandwith RS232 interface.

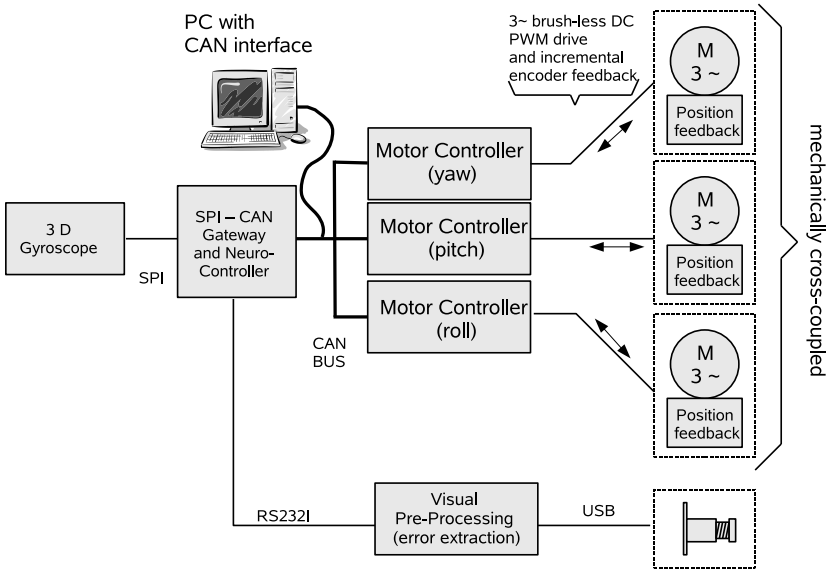

Figure 9. System overview and adapted connectivity. The central element is the embedded neuro-processor and gateway board.

3. A Mechatronic Testbed

3.1. Mechanical Setup

Since it is the VOR's task to stabilise gaze when the head undergoes rotational perturbations, we designed a platform which can artificially induce them in a controlled manner. To be clear, the platform is a completely independent system that is driven by a separate embedded system. The mechatronic eye sits on top of this platform and uses only the gyroscopes to obtain information about rotational velocities.

The gyroscopic information is then used to drive the oculomotor plant as described in section 2.1. If the rotational velocity of the eye does not match the required velocity, the vision system experiences slip. It is this error signal that the learning algorithm (see section 4) uses to tune the adaptive filter which models the cerebellar cortex.

¶ CAN is a broadcast, differential signal 2-wire bus developed by BOSCH^{TM}for communication between control units in automobiles but is now widely used in distributed embedded systems.

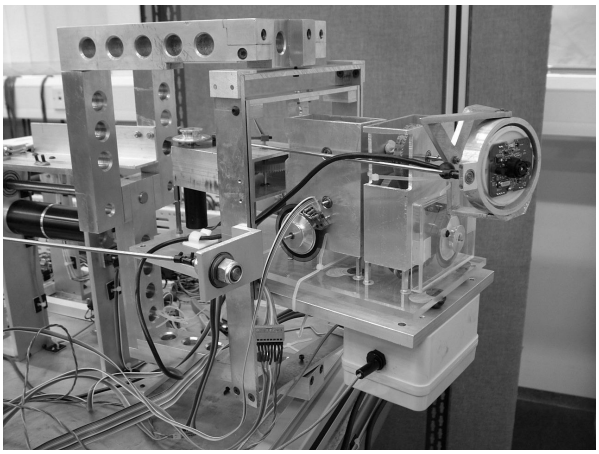

Figure 10. The mechatronic eye is placed on a platform which can be driven by an independent controller. The gyroscope is placed under the platform (grey box).

3.1.1. Non-linearities in the oculomotor system In biology, as well as in our engineering system, three sources of nonlinearities can easily be identified: (a) actuator nonlinearities, (b) visual distortion due to lens shape and (c) off-axis effects. The main potential source for non-linearities in our system are the off-axis effects due to non-coinciding axes of rotation for the eye and the head, respectively. If the head is rotated, the eye not only experiences this rotation but it is also translated in the horizontal plane (see figure 11).

Given a certain angle of head rotation, the eye is therefore required to turn the equivalent amount (in the opposing direction) plus an additional corrective angle $\phi_{Corr.}$ (see equation 5), in order to maintain gaze on the target.

$$\phi_{Eye} = -(\phi_{Corr.} + \phi_{Head}) \tag{4}$$

The ratio of distance from the eye to the target (d) and the distance from the head axis to the eye axis (a) determines the degree of non-linearity. For $d \to \infty$ or $a \to 0$ the system is linear and no correction is required.

$$\phi_{Corr.} = \arctan\left(\frac{a \cdot \sin\phi_{Head}}{d + a \cdot (1 - \cos\phi_{Head})}\right) \tag{5}$$

Figure 12 shows the required corrective angle $\phi_{Corr.}$ for different $\frac{d}{a}$ ratios. The solid line represents our experimental conditions ($a = 0.2m$ and $d = 1.37m$) and it can be seen that in this case the system can be understood as quasi-linear. Consequently, equation 4 simplifies to

$$\phi_{Eye} \approx g_{Corr.} \cdot \phi_{Head} \tag{6}$$

with $g_{Corr.}$ representing the slope of the solid graph in figure 12. Analytically, $g_{Corr.}$ can be understood as the first order parameter of the Taylor series of equation 4 with a base point of zero ($g_{Corr.} = 1 + \frac{a}{d} = 1.146$).

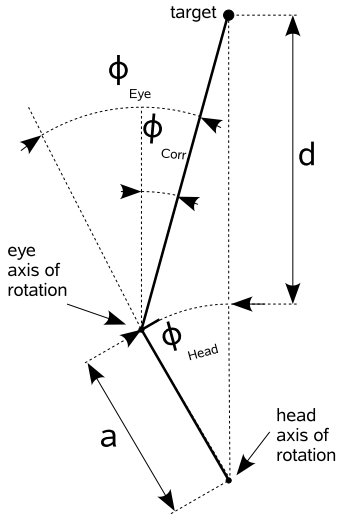

Figure 11. Non-coinciding axes of rotation for head and eye cause system non-linearities. A head rotation of ϕ_{Head} from the vertical requires an equivalent eye rotation (in the opposite direction) plus a corrective rotation ϕ_{Corr} in order to achieve stable gaze on the stationary target.

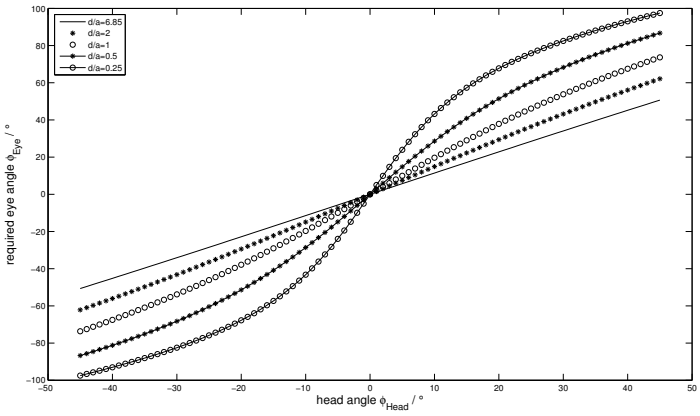

Figure 12. The non-linearities are a function of the ratio d over a.

4. On-Line Learning Algorithm

In order to reduce the perceived visual slip from the gyroscopic input, we have to change the weights of the adaptive filter. These weights represent the parallel fibre Purkinje cell synapses of the cerebellar cortex. The successful application of this on-line learning algorithm should tune the weights in such a manner that the cerebellum, in conjunction with the brainstem, are dynamically equivalent to the inverted oculomotor plant.

$$e(t) = (P - B^{-1} + C) \cdot y(t). \tag{7}$$

As observable in equation 7, the error is reduced to zero when $C = B^{-1} - P$. Here, the advantage of the recurrent structure becomes apparent. The sensory error $e(t)$ is a direct consequence of the output of the adaptive filter structure C. Effectively, this learning topology therefore does not require a translation of the sensory error into a motor-command error. Consequently, the perceived visual slip is expected to form an appropriate teaching signal for the adaptation of the filter.

To achieve this, the weights (w_i) of the FIR filter representing C (see equation 3) are altered using a simple gradient descent approach:

$$\delta w_i = -\beta \cdot y_{i+k}(t) \cdot sign(e(t)) \tag{8}$$

Here, it is important to note that the learning algorithm takes into account the delay of the vision signal. Since the error observed at time t was caused by events at time $t - 100ms$, the required change of the set of filter weights must be based on the current error and on each weight-path's input state when erroneous output was generated. This is reflected in equation 8 by changing the weight w_i in proportion to filter tap y_{i+k}. The delay constant k expresses the error delay in multiples of the filter's unit delay. In our case $k = \frac{t_{VisionDelay}}{\Delta T} = \frac{100ms}{10ms} = 10$.

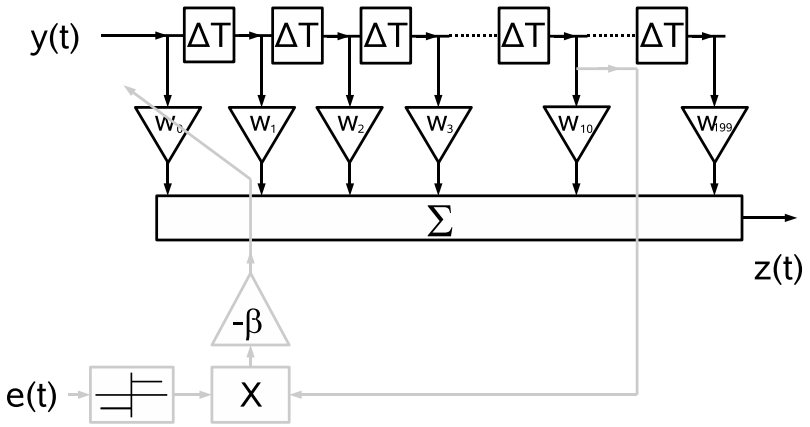

Figure 13. An illustration of the delayed gradient descent learning rule. In this example the weight w_0 is changed based on the sign of the current error ($e(t)$) and the input into w_0 when the error was caused 100ms ago. This input has moved through the filter and is currently present as an input for w_{10}. The unit delay (ΔT) of the filter is 10ms. The solid black parts of the figure represent the feed-forward path and the light grey routes refer to the learning algorithm as described in equations 8 and 3).

In other words, for each time step the change in weight is proportional to its associated delayed tap contribution to the error. The direction of change is governed by the sign of this error. The learning rate is fixed and defined by constant β. The weight change takes place on-line and continuously as long as visual slip exists.

4.1. Implementation Issues

We believe that for the successful application of many parallel adaptive neural control structures in multi-degree of freedom systems (i.e. the task that the cerebellum seems to perform), it is crucial that the computational requirements are reduced to a minimum. We have therefore implemented our algorithm purely in fixed-point arithmetic. The 200 weights are stored as signed 32-bit integers and the input history $y(t)$ is represented as a 16-bit integer. Before calculating the weighted sum, the weight values are right shifted by 16 bits. This assures that the smallest possible increment in weight is $\frac{1}{2^{16}}$ of the resolution of the motor command $y(t)$. This constitutes an effective measure to achieve a learning rate $\beta \ll 1$, which is crucial for slow and stable learning in a fixed point algorithm.

5. Experimental Results

To test the effectiveness of the algorithm, the platform is driven with a band-passed random signal (see figure 14) which is similar to the typical horizontal head rotations experienced by humans during locomotion [12].

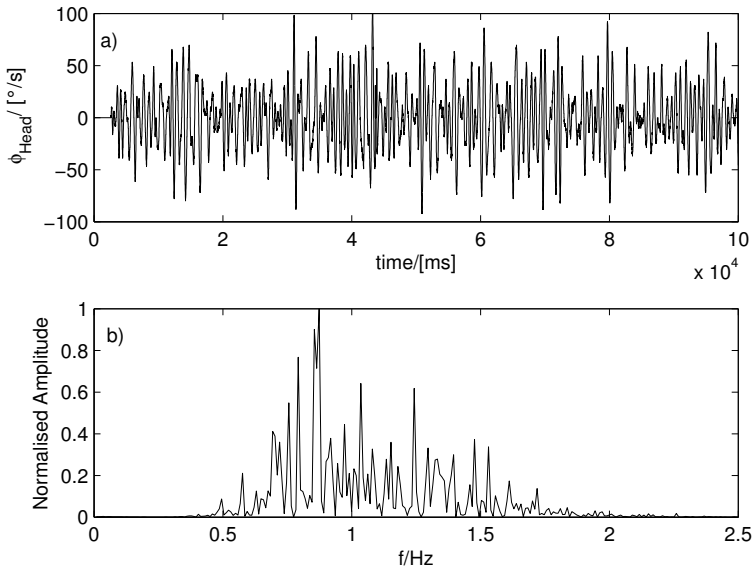

Figure 14. Rotational velocities of platform as a function of time (a) and corresponding spectrum (b).

Since in the untrained system (all cerebellar weights are set to zero on startup), the brainstem filter alone does not generate a signal that matches the required oculomotor drive signal, the eye and head velocities do not match, as shown in figure 15. However, after a few minutes, the learning algorithm has tuned the cerebellum in such a way that,

in conjunction with the brainstem, the visual slip is reduced significantly, with eye and head velocities matching almost perfectly (see figure16).

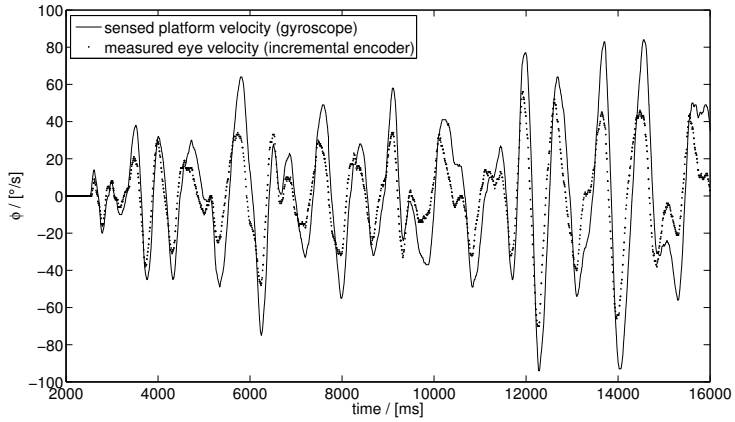

Figure 15. Brainstem circuitry alone can only partially reduce the visual slip and consequently head and eye velocities do not match.

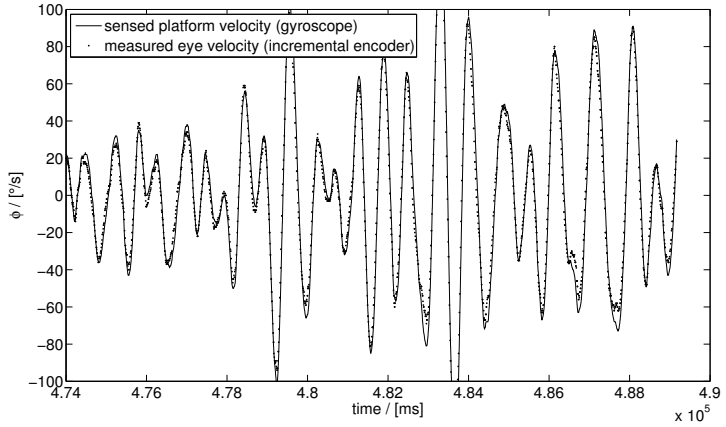

Figure 16. A well tuned cerebellum causes an almost perfect match of head and eye velocity.

It should, again, be noted that the system does not operate as a closed loop system and the correct drive signal is generated by the brainstem-cerebellar structure in a feed-forward manner. The sign of the (delayed) vision system is only used as a 'soft' training signal which constantly tunes the cerebellum.

In a second set of experiments, the cerebellar structure is trained to drive an oculomotor plant with a time constant of 50 ms. Once the filter weights have converged, the plant dynamics are changed to 100 ms and the cerebellum's task is to adapt to the plant variation. To be clear, the data shown below (visual slip, figure 17) is again from

the real oculomotor system on the platform. We made use of the flexible motor control structure as described in section 2.2.2 to induce this sudden change in system dynamics.

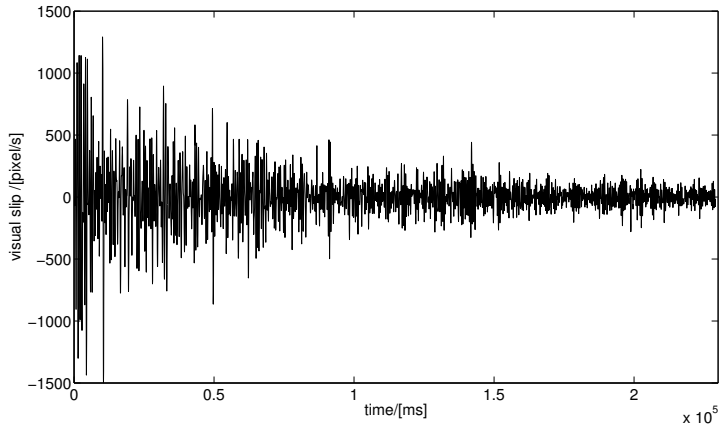

Figure 17. The Vision system experiences image motion after the plant dynamics have changed. Over time, the slip is notably reduced.

To quantitatively display the improvement, the root-mean square (RMS, figure 18) of the visual slip is calculated over 600 samples$^+$, normalised and plotted. The reduction of the visual slip is clearly visible.

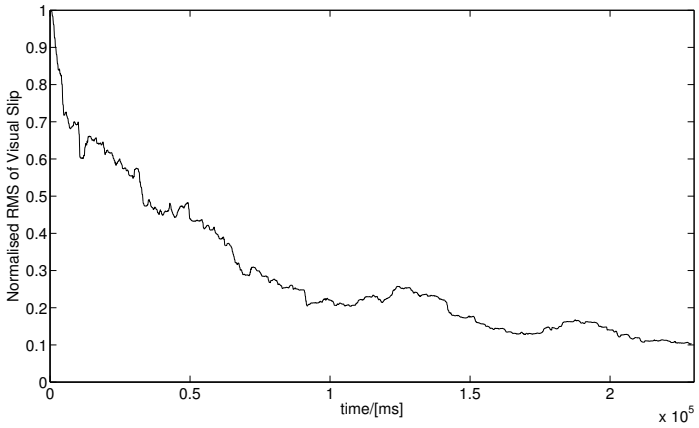

Figure 18. Normalised RMS of visual slip. Cerebellar training reduces the visual slip by approximately 90% .

$^+$ The sample length is a somewhat arbitrary choice and represents 20 seconds with a 30 frames per second camera.

6. Discussion and Further Work

In the previous sections we have shown how a biologically inspired recurrent adaptive control algorithm can successfully improve the performance of a robotic implementation of a mammalian reflex, namely the VOR. The architecture is able to adapt to dynamic changes of a mechatronic system in an on-line training architecture, which is of great importance for reliable autonomous robots so that they can continue to operate accurately under changing payloads or in the face of degrading components.

The latency in biological vision systems, as well as in other proprioceptive signals, forces organisms to adopt an open-loop approach for the vast majority of their motor functions. This differs greatly from conventional engineering approaches where closed-loop control is the most common control scheme. However, we still believe that the engineering community can benefit from this alternative solution.

We have shown that the training signal, in our case vision, can be of a very basic nature. In our case, only the sign of the error is sufficient to tune the feed-forward filter. This fact could be exploited in at least two possible ways: firstly, very economical sensors are possible and secondly, since the necessary information could be encoded in only two bits (positive signal, negative signal, no signal) low bandwidth transmission is possible. Another advantage of the proposed architecture is its capability to deal with a delayed feedback signal. Such a delay could be encountered when remotely sensing over long distances or if a large amount of pre-processing is required to extract feedback data from a convoluted source. When the latency of the error signal is known, the learning algorithm can take this into account by adjusting the weights based on the filter state when the erroneous drive signal was created, instead of using the filter state when the error signal is received. Using a highly delayed error signal directly in a closed-loop controller is a potential source for instabilities and would only work for low frequency stimulation.

The choice of a very slow learning rate, and therefore adaptation times of 10 to 20 minutes, brings with it the advantage that even quite noisy sensory signals can be used to train the adaptive filter. As long as the noise is truly random, weight changes due to noise cancel each other out over time. As a result, only relevant information of the error feedback signal contributes in the long term to the tuning of the weights. Again, very noisy feedback signals are prohibitive in closed-loop control schemes.

The fact that the adaptive algorithm could successfully be implemented on a medium range microcontroller in fixed point arithmetic suggests a potential for cost-driven mass market applications.

In our further work we are currently addressing a second site of plasticity which is suggested to exist in the brainstem. Naturally, we also aim to extend the control scheme for pitch and roll perturbations and to investigate the cross coupling of three dimensional movements. As an alternative actuation scheme for the oculomotor system, we have just developed an air muscle driven system, and will explore the ability of our algorithm to deal with this inherently non-linear plant.

References

[1] Michael E. Goldberg. *Principles of Neural Science*, chapter The Control of Gaze, pages 782–798. McGraw-Hill, New York, 4th edition, 2000.

[2] Masao Ito. Cerebellar learning in the vestibulo-ocular reflex. *Trends in Cognitive Sciences*, 2(9):313–321, September 1998.

[3] Dianne M. Broussard and Charles D. Kassardjian. Learning in a simple motor system. *Learning and Memory*, 11:127–136, 2004.

[4] Claude Ghez and W. Thomas Thach. *Principles of Neural Science*, chapter The Cerebellum, pages 832–852. McGraw-Hill, New York, 4th edition, 2000.

[5] David Marr. A theory of cerebellar cortex. *Journal of Physiology*, pages 437–470, 1969.

[6] James S. Albus. A theory of cerebellar function. *Mathematical Biosciences*, 10:25–61, 1971.

[7] Masao Ito. *The cerebellum and neural control*. Raven Press, New York, 1984.

[8] Paul Dean, John Porrill, and James V. Stone. Decorrelation control by the cerebellum achieves oculomotor plant compensation in simulated vestibulo-ocular reflex. *Proc. R. Soc. Lond.*, (269):1895–1904, 2002.

[9] John Porrill, Paul Dean, and James V. Stone. Recurrent cerebellar architecture solves the motor-error problem. *Proceedings of the Royal Society of London*, 2004.

[10] Mitsuo Kawato. *Feedback-Error-Learning Neural Network for Supervised Motor Learning*, pages 365–372. North-Holland, Amsterdam, 1990.

[11] T. Shibata and S. Schaal. Biomimetic gaze stabilization based on feedback-error-learning with nonparametric regression networks. *Neural Networks*, (14):201–216, 2001.

[12] G. Grossman and R. Leigh et al. Frequency and velocity of rotational head perturbations during locomotion. *Experimental Brain Research*, (70):470–476, 1988.

Acknowledgements

This work has been partially funded by EPSRC grant GR/T10602/01. We thank our collaborators Paul Dean, John Porrill and Sean Anderson (University of Sheffield) as well as Mayank Dutia and John Menzies (University of Edinburgh) for useful discussions and inspiration.